J Eng Math (2021) 128:9
https://doi.org/10.1007/s10665-021-10133-3

An asymptotic investigation of the dynamics and dispersion of an elastic five-layered plate for anti-plane shear vibration

R. Nawaz · Rahmatullah Ibrahim Nuruddeen · Q. M. Zaigham Zia

Received: 17 April 2020 / Accepted: 1 November 2020 / Published online: 12 May 2021

Abstract An asymptotic approach of analysis is used to analyze the antisymmetric anti-plane shear dispersion of an elastic inhomogeneous five-layered plate in the presence of material contrasts. The resultant exact dispersion relation, overall cut-off frequency and the low-frequency range are determined. Two different asymptotic contrasting material setups for layered plates are employed with regards to the optimal shortened polynomial dispersion relation in the context of the structure under consideration. The asymptotic behaviors of the displacements and stresses in the respective layers of the plate are also examined. Finally, we provided some concluding remarks.

Keywords Asymptotic approach · Composite layered plates · Contrasting setups · Inhomogeneous plate

1 Introduction

Wave propagations in elastic materials have been studied extensively in the literature [1–3] due to their frequent occurrence in many engineering applications and structures. Notable among these structures and devices where the wave propagation is of great interest include the waveguide devices [4,5], elastic beams and sandwich beams [6,7], photovoltaic panels and laminated glass [8], elastic sandwich plates [9] and multi-layered and composite plates of different configurations [10–22] to mention a few. In general, multilayered structures have advantages of high resistance, weightlessness, and strength due to the presence of many layers that are made from different materials; besides, they also possess static and dynamic excitations. Further, different methods have been employed in the above-cited papers comprising of analytical, computational and asymptotic approaches to analyze the dispersion and propagation of elastic and surface waves in layered structures. For instance, a plane shear problem of inhomogeneous three-layered laminates and an anti-plane shear problem of strongly inhomogeneous three-layered infinite plates were recently analyzed with the help of an asymptotic analysis approach in [10] and [11,12], respectively. Also, in references [10–12], a complete analysis of the analytically obtained dispersion relation was carried out in relation to the approximate one amidst the presence of material contrasts. This analysis was directed towards exploring the exactness of the shortened approximate dispersion relations to the analytical ones in the presence of these contrasts

R. Nawaz (✉)· R. I. Nuruddeen · Q. M. Z. Zi
Department of Mathematics, COMSATS University Islamabad, Islamabad 44000, Pakistan
e-mail: rabnawaz@comsats.edu.pk

R. I. Nuruddeen
Department of Mathematics, Faculty of Science, Federal University Dutse, Jigawa 7156, Nigeria

and under long-wave low-frequency behavioral assumption. Similar consideration with regards to the elastic rods and multi-component elastic structures can be seen in [13] and [14], correspondingly; while [15] investigated the effects of viscous damping on the propagation of elastic waves in inhomogeneous layered plates and [16] examined the significance of certain external excitations on the wave propagation in a layered plate; see also [17,18] for other deliberation regarding laminated composite plates and circular nanoplates. Peculiarly, since we are examining a five-layered plate in the present manuscript due to their vast applications in modern technology, authors in [19–22] have examined various configurations for five-layered plates; a number of relevant studies on the five-layered plate include the application of the Navier's method to analyze a five-layered sandwich plate with viscoelastic core layers [19], the analysis of static and dynamic effects in a five-layered glass plate [20], the stress analysis of a five-layered sandwich composite based on the shear deformation theories [21], and the asymptotic investigation with regards to the dispersion of elastic waves in a strongly non-homogeneous five-layered plate [22]. Emphasizing on [22], the layer configuration required the introduction of a unification procedure for the complete analysis of the four contrasting material setups to take place. In the same vein, for more on the elastic wave propagation in other layered and composite media, see [23–42] and the references therein.

However, in this paper, we examine the anti-plane shear vibration of an isotropic five-layered plate composed of three different layers of varying material properties. The plate which is of infinite extent is considered to be in a symmetrical form. By symmetry here, one decides to analyze either the symmetric or antisymmetric modes. Nevertheless, we consider the antisymmetric vibration mode having satisfied the global low-frequency regime. Further, the resultant dispersion relation and its corresponding polynomial dispersion relation are set to be analyzed. The two contrasting material setups [10–12] would be investigated within the long-wave low-frequency estimates. In addition, the asymptotic behaviors of the displacements and stresses in the respective layers will be examined. Further, the paper is organized as follows: In Sect. 2, we give the general formulation of the problem and outlined the two setups to be analyzed. Section 3 gives the exact solution of the formulated problem. The exact dispersion relation and the cut-off frequency are determined in Sect. 4. The shortened polynomial dispersion analyses in connection to contrasting setups are given in Sect. 5. We give the asymptotic behaviors of the related quantities in Sect. 6; while Sect. 7 gives the conclusion.

2 Problem formulation

Consider an anti-plane shear vibration of an isotropic five-layered plate including the inner core of thickness $2h_1$, the outer core layers of thicknesses h_2 and the skin layers of thicknesses h_2 placed respectively symmetrical about the mid-point as shown in Fig. 1 below. The inner core and skin layers are assumed to be of the same material constituents.

The equations of motion in (x_1, x_2) describing the vibration in the respective layers of the plate take the following form

$$\frac{\partial \sigma_{13}^{i}}{\partial x_1} + \frac{\partial \sigma_{23}^{i}}{\partial x_2} = \rho_i \frac{\partial^2 U_i}{\partial t^2}, \quad i = 1, 2, 3, \tag{1}$$

where x_n $(n = 1, 2)$ are the spatial variables, t is the temporal variable, U_i are the out of plane displacements for $i = 1, 2, 3$ standing for the inner core layer, outer core layers and the skin layers, accordingly. It is also important to note that the inner core layer and the skin layers are considered to be of the same materials. Further, the shear stresses σ_{j3}^{i} $(i = 1, 2, 3)$ are defined respectively as follows:

$$\sigma_{j3}^{i} = \mu_i \frac{\partial U_i}{\partial x_j}, \quad j = 1, 2, \tag{2}$$

where μ_i are the Lame's elastic constants of motion. We also prescribe the following continuity conditions comprising of the continuity of displacements and stresses along the interfaces of the respective layers

(a) $U_1(x_1, x_2, t) = U_2(x_1, x_2, t)$ at $x_2 = \pm h_1$,

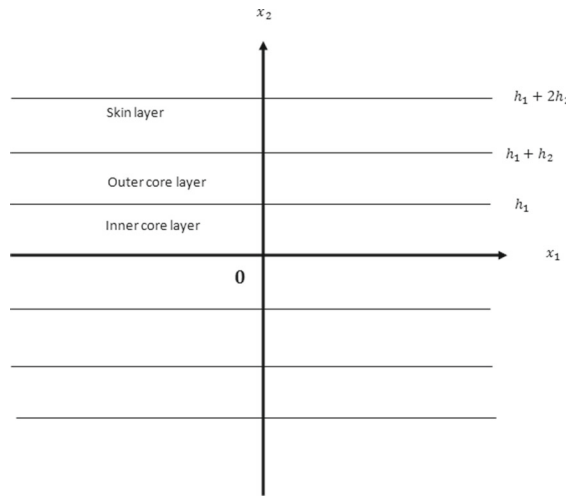

Fig. 1 A symmetric five-layered plate

(b) $\sigma_{23}^{1}(x_1, x_2, t) = \sigma_{23}^{2}(x_1, x_2, t)$ at $x_2 = \pm h_1$,
(c) $U_2\,(x_1, x_2, t) = U_3\,(x_1, x_2, t)$ at $x_2 = \pm(h_1 + h_2)$,
(d) $\sigma_{23}^{2}(x_1, x_2, t) = \sigma_{23}^{3}(x_1, x_2, t)$ at $x_2 = \pm(h_1 + h_2)$, (3)

and the traction-free conditions on the outer faces as follows:

(e) $\sigma_{23}^{3}(x_1, x_2, t) = 0$ at $x_2 = \pm(h_1 + 2h_2)$. (4)

However, in this paper, we investigate the possibilities of obtaining optimal estimate or rather the range for the best dimensionless parameters leading to the approximate fundamental mode with a zero cut-off frequency in relation to the inhomogeneous strongly five-layered plate under the two contrasting material setups given by the following asymptotic relations [10–12]:

$$\begin{cases} \text{(i)} \;\; \mu \ll 1, \;\; h \sim 1, \;\; \rho \sim \mu, \\ \\ \text{(ii)} \; \mu \ll 1, \;\; h \sim \mu, \;\; \rho \sim \mu^2, \end{cases} \tag{5}$$

of which (i) corresponds to a three-layered plate with stiff skin layers and light core layer and (ii) matches with a three-layered plate with stiff thin skin layers and light core layers, respectively. More importantly, the same asymptotic relations for the three-layered plate given in Eq. (5) will be utilized to investigate the approximate dispersion relation for the anti-plane shear vibration of the five-layered plate under consideration by suitably sandwiching the three-layered plate [11,12] between new skin layers (above and below) of similar material constituents with that of the core layer of the three-layered plate. In fact, this will not cause us to devise a different means of showcasing Eq. (5). In addition, in a multi-layered or composite structure; it is important to note that no two successive layers are exactly made of the same materials otherwise you have no multi-layer. It is also noteworthy to mention here that [22] analyzed a strongly inhomogeneous five-layered plate with entirely dissimilar layers that requires the introduction of a unification procedure for the complete analysis; whereas in the present study, the plate is considered to be of alternating layers similar to the recently investigated elastic beams [6]. More, the present consideration preserves the nature of the contrasting setups given in Eq. (5); that is, we need not to unify the dimensionless parameters before proceeding to the aiming analysis.

3 Exact solution

We determine the exact analytical solution of the formulated problem. In doing so, the displacements and stresses of the respective layers will be determined from Eqs. (1)–(4). Thus, we get from Eqs. (1) and (2) the following wave equation:

$$\frac{\partial^2 U_i}{\partial x_1^2}+\frac{\partial^2 U_i}{\partial x_2^2}=\frac{1}{c_i^2}\frac{\partial^2 U_i}{\partial t^2},\quad i=1,2,3, \tag{6}$$

where $c_i=\sqrt{\mu_i/\rho_i}$ is the transverse speed with $c_1=c_3$ having assumed that the inner core layer and the skin layers to be of same material. Now, since the plate is symmetric, and with the harmonic solution assumption of the form

$$U_i(x_1,x_2,t)=u_i(x_2)\mathrm{e}^{\mathrm{i}(kx_1-\omega t)}, \tag{7}$$

the solutions of Eq. (6) in the inner core layer, outer core layer and the skin layer are determined as forms

$$\begin{cases} u_1(x_2)=A_1\cosh\left(\sqrt{k^2-\frac{\omega^2}{c_1^2}}x_2\right)+B_1\sinh\left(\sqrt{k^2-\frac{\omega^2}{c_1^2}}x_2\right), & 0\le x_2\le h_1,\\ u_2(x_2)=A_2\cosh\left(\sqrt{k^2-\frac{\omega^2}{c_2^2}}x_2\right)+B_2\sinh\left(\sqrt{k^2-\frac{\omega^2}{c_2^2}}x_2\right), & h_1\le x_2\le h_1+h_2,\\ u_3(x_2)=A_3\cosh\left(\sqrt{k^2-\frac{\omega^2}{c_1^2}}x_2\right)+B_3\sinh\left(\sqrt{k^2-\frac{\omega^2}{c_1^2}}x_2\right), & h_1+h_2\le x_2\le h_1+2h_2, \end{cases} \tag{8}$$

where $\mathrm{i}=\sqrt{-1}$, k is the wave number, and ω is the frequency. Furthermore, the formulated problem via the solutions obtained in Eq. (8) coupled to the boundary conditions in Eqs. (3) and (4) give the following dimensionless displacements and stresses in the respective layers of the symmetric five-layered plate after omitting the exponential factors as follows:

$$\begin{aligned} u_1&=h_2\frac{\sinh\left(\alpha_2 h\xi_{2_1}\right)}{\alpha_2},\\ \sigma_{13}^1&=\mathrm{i}\mu_1 K\frac{\sinh\left(\alpha_2 h\xi_{2_1}\right)}{\alpha_2},\\ \sigma_{23}^1&=\mu_1\cosh\left(\alpha_2 h\xi_{2_1}\right), \end{aligned} \tag{9}$$

$$\begin{aligned} u_2&=\frac{h_2}{\alpha_2}\left(\sinh\left(\alpha_2 h\right)\cosh\left(\alpha_1\xi_{2_2}\right)+\Gamma\cosh\left(\alpha_2\right)\sinh\left(\alpha_1\xi_{2_2}\right)\right),\\ \sigma_{13}^2&=\mathrm{i}\mu_2\frac{K}{\alpha_2}\left(\sinh\left(\alpha_2 h\right)\cosh\left(\alpha_1\xi_{2_2}\right)+\Gamma\cosh\left(\alpha_2\right)\sinh\left(\alpha_1\xi_{2_2}\right)\right),\\ \sigma_{23}^2&=\mu_2\frac{\alpha_1}{\alpha_2}\left(\sinh\left(\alpha_2 h\right)\sinh\left(\alpha_1\xi_{2_2}\right)+\Gamma\cosh\left(\alpha_2\right)\cosh\left(\alpha_1\xi_{2_2}\right)\right), \end{aligned} \tag{10}$$

and

$$\begin{aligned} u_3&=h_2\Theta\left(\cosh\left(\alpha_2\left(\xi_{2_3}+h+1\right)\right)-\tanh\left(\alpha_2\left(h+2\right)\right)\sinh\left(\alpha_2\left(\xi_{2_3}+h+1\right)\right)\right),\\ \sigma_{13}^3&=i\mu_1 K\Theta\left(\cosh\left(\alpha_2\left(\xi_{2_3}+h+1\right)\right)-\tanh\left(\alpha_2\left(h+2\right)\right)\sinh\left(\alpha_2\left(\xi_{2_3}+h+1\right)\right)\right),\\ \sigma_{23}^3&=\mu_1\alpha_2\Theta\left(\sinh\left(\alpha_2\left(\xi_{2_3}+h+1\right)\right)-\tanh\left(\alpha_2\left(h+2\right)\right)\cosh\left(\alpha_2\left(\xi_{2_3}+h+1\right)\right)\right), \end{aligned} \tag{11}$$

where

$$\Gamma=\frac{\alpha_2}{\alpha_1\mu},\ \Theta=\frac{\cosh\left(\alpha_2(h+2)\right)}{\alpha_2\cosh\left(\alpha_2\right)}(\cosh\left(\alpha_1\right)\sinh\left(\alpha_2 h\right)+\Gamma\sinh\left(\alpha_1\right)\cosh\left(\alpha_2 h\right)), \tag{12}$$

coupled to the corresponding scaled variables

$$\begin{aligned} \xi_{2_1}&=\frac{x_2}{h_1}, && 0\le x_2\le h_1,\\ \xi_{2_2}&=\frac{x_2-h_1}{h_2}, && h_1\le x_2\le h_1+h_2,\\ \xi_{2_3}&=\frac{x_2-(h_1+h_2)}{h_2}, && h_1+h_2\le x_2\le h_1+2h_2. \end{aligned} \tag{13}$$

with

$$\begin{cases} \alpha_1 = \sqrt{K^2 - \Omega^2}, \\ \alpha_2 = \sqrt{K^2 - \frac{\mu}{\rho}\Omega^2}, \end{cases} \tag{14}$$

and the dimensionless frequency Ω and wave number K given by

$$\begin{cases} \Omega = \frac{\omega h_2}{c_2}, \\ K = k h_2, \end{cases} \tag{15}$$

together with the following dimensionless parameters:

$$\begin{cases} \mu = \frac{\mu_2}{\mu_1}, \\ h = \frac{h_1}{h_2}, \\ \rho = \frac{\rho_2}{\rho_1}. \end{cases} \tag{16}$$

4 Asymptotic approach to exact dispersion relation

In this section, the exact dispersion relation and cut-off frequency of the given formulated problem are determined. Also, the this dispersion relation will further be approximated to its corresponding polynomial dispersion relation for onward analysis in the subsequent section. Therefore, the exact analytical solution of the symmetric plate determined in Eq. (8) coupled to the boundary conditions given in Eqs. (3) and (4) posed a 5×5 dispersion matrix of such after dimensionalizing results in

$$\begin{vmatrix} \sinh(h\alpha_2) & -\cosh(h\alpha_1) & -\sinh(h\alpha_1) & 0 & 0 \\ \Gamma\cosh(h\alpha_2) & -\sinh(h\alpha_1) & -\cosh(h\alpha_1) & 0 & 0 \\ 0 & \cosh((h+1)\alpha_1) & \sinh((h+1)\alpha_1) & -\cosh((h+1)\alpha_2) & -\sinh((h+1)\alpha_2) \\ 0 & \sinh((h+1)\alpha_1) & \cosh((h+1)\alpha_1) & -\Gamma\sinh((h+1)\alpha_2) & -\Gamma\cosh((h+1)\alpha_2) \\ 0 & 0 & 0 & \sinh((h+2)\alpha_2) & \cosh((h+2)\alpha_2) \end{vmatrix} = 0, \tag{17}$$

where Γ is given in Eq. (12) with the dimensionless parameters defined in Eqs. (14)–(16).

Thus, the *exact dispersion relation* is obtained from Eq. (17) to be

$$\begin{aligned} &\alpha_1^2\mu^2 \sinh(\alpha_1)\cosh(\alpha_2)\sinh(\alpha_2 h) + \alpha_2\alpha_1\mu\cosh(\alpha_1)\cosh(\alpha_2(h+1)) \\ &+\alpha_2^2 \sinh(\alpha_1)\sinh(\alpha_2)\cosh(\alpha_2 h) = 0, \end{aligned} \tag{18}$$

with the following *cut-off frequency* at $K = 0$ from Eq. (18) as follows:

$$\begin{aligned} &\sin(\Omega)\sin\left(\sqrt{\frac{\mu}{\rho}}\Omega\right)\cos\left(h\sqrt{\frac{\mu}{\rho}}\Omega\right) - \sqrt{\mu\rho}\cos(\Omega)\cos\left((h+1)\sqrt{\frac{\mu}{\rho}}\Omega\right) \\ &+\mu\rho\sin(\Omega)\cos\left(\sqrt{\frac{\mu}{\rho}}\Omega\right)\sin\left(h\sqrt{\frac{\mu}{\rho}}\Omega\right) = 0. \end{aligned} \tag{19}$$

From Eq. (19), we get the predicted single cut-off frequency as

$$\Omega \approx \sqrt{\frac{\rho}{rh}} \ll 1, \tag{20}$$

over the low-frequency range

$$\frac{\rho}{r} \ll h \ll \frac{r}{\mu}, \tag{21}$$

where

$$r = 1 + \mu\rho.$$

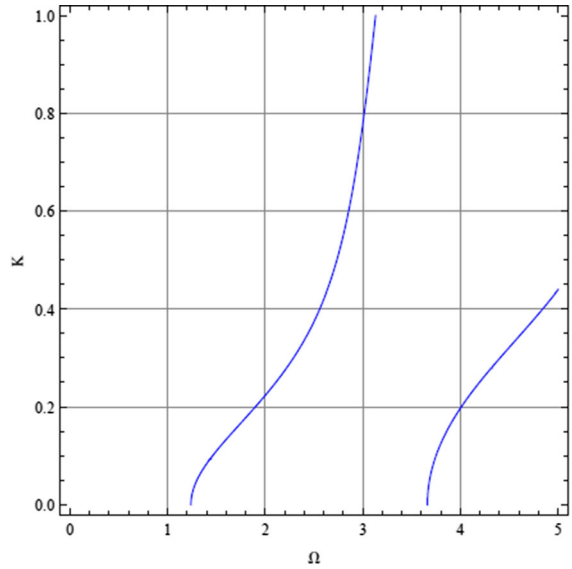

Fig. 2 Dispersion curves from Eq. (18) for the non-estimated range case with the following parameters: $\mu = 0.025$, $\rho = 0.03$, $h = 1.0$

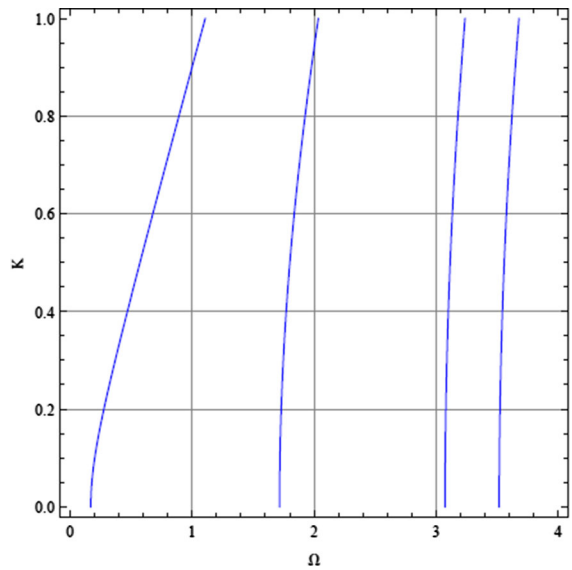

Fig. 3 Dispersion curves from Eq. (18) for the estimated range case with the following parameters: $\mu = 0.025$, $\rho = 5.97$, $h = 4.0$

It is clear from Eqs. (20) and (21) that when $r = 1$ the predicted single cut-off frequency found in [11,12] with regards to predicted single cut-off frequency and low-frequency range for the three-layered laminate is recovered. More so, we mention here that the low-frequency is attained when $\Omega \ll 1$, while the long wave vibration is achieved when $K \ll 1$, [2,10].

Dispersion curves from the exact dispersion relation Eq. (18) is plotted in Fig. 2 for the non-estimated range and Fig. 3 for the estimated range of zero cut-off frequencies, respectively. As anticipated, the cut-off frequency is not observed in Fig. 2 since the choice of parameters is outside the estimated range given in Eq. (21); while lowest low-frequency is achieved in Fig. 3 over the stated range.

4.1 Polynomial dispersion relation

The polynomial dispersion relation is determined from the exact dispersion relation given in Eq. (18) by the application of Taylor's series expansion as follows:

$$\mu + \chi_1 K^2 + \chi_2 K^4 + \chi_3 K^2\Omega^2 + \chi_4\Omega^2 + \chi_5\Omega^4 + \cdots = 0 \tag{22}$$

with

$$\begin{aligned}
\chi_1 &= \frac{h^2\mu}{2} + h\mu^2 + h\mu + \mu + 1,\\
\chi_2 &= \frac{h^3\mu^2}{6} + \frac{h^2\mu}{4} + \frac{h^2}{2} + \frac{2h\mu^2}{3} + \frac{h\mu}{2} + \frac{7\mu}{24} + \frac{1}{3},\\
\chi_3 &= -\frac{h^3\mu^3}{6\rho} - \frac{1}{6}h^3\mu^2 - \frac{h^2\mu^2}{4\rho} - \frac{h^2\mu}{\rho} - \frac{h^2\mu}{4} - \frac{h\mu^3}{2\rho} - \frac{h\mu^2}{2\rho} - \frac{5h\mu^2}{6} - \frac{h\mu}{2} - \frac{\mu^2}{4\rho} - \frac{\mu}{2\rho} - \frac{\mu}{3} - \frac{1}{6},\\
\chi_4 &= -\frac{h^2\mu^2}{2\rho} - \frac{h\mu^2}{\rho} - h\mu^2 - \frac{\mu^2}{2\rho} - \frac{\mu}{\rho} - \frac{\mu}{2},\\
\chi_5 &= \frac{h^3\mu^3}{6\rho} + \frac{h^2\mu^2}{2\rho^2} + \frac{h^2\mu^2}{4\rho} + \frac{h\mu^3}{2\rho} + \frac{h\mu^2}{2\rho} + \frac{h\mu^2}{6} + \frac{\mu^2}{6\rho^2} + \frac{\mu^2}{4\rho} + \frac{\mu}{6\rho} + \frac{\mu}{24},\\
&\vdots
\end{aligned} \tag{23}$$

5 Shortened polynomial dispersion relations

In this section, we approximate the obtained polynomial dispersion relation in Eq. (22) in connection to the two contrasting material setups given in Eq. (5) to obtain the corresponding optimal shortened polynomial dispersion relation in each setup. However, having sandwiched the three-layered plate [9–11] in between new skin layers below and above of similar material constituents with that of the core layer of the three-layered plate; the asymptotic relations in Eq. (5) under the current plate correspond to (i) a five-layered plate with stiff skin layers, light outer core layers and stiff inner core layer; and (ii) a five-layered plate with stiff thin skin layers, light outer core layers and stiff thin inner core layer. We thus investigate the roles of these setups on the anti-plane shear vibration of a five-layered plate in this section.

5.1 Stiff skin layers, light outer core layers and stiff inner core layer ($\mu \ll 1,\ h \sim 1,\ \rho \sim \mu$)

Here, both the skin layers and the inner core layer are made up of the same stiff material while the outer core layers are made up of a light material, that is, the five-layered plate is made of alternating stiff-light layers, (almost similar consideration is made in the subsequent case, but with stiff thin skin and stiff thin inner core layers).

Thus, on using the present setup, it can be seen from Eq. (23) that the following asymptotic relation:

$$G_1 \sim G_2 \sim G_3 \sim G_4 \sim G_5 \sim 1, \tag{24}$$

and having in mind that higher orders of μ go to zero more faster, we obtain the following by retaining only μ

$$\begin{aligned}
G_1 &= \frac{5\mu}{2} + 1,\\
G_2 &= \frac{25\mu}{24} + \frac{5}{6},\\
G_3 &= \left(-\mu - \frac{3}{2}\right)\nu - \frac{13\mu}{12} - \frac{1}{6},
\end{aligned}$$

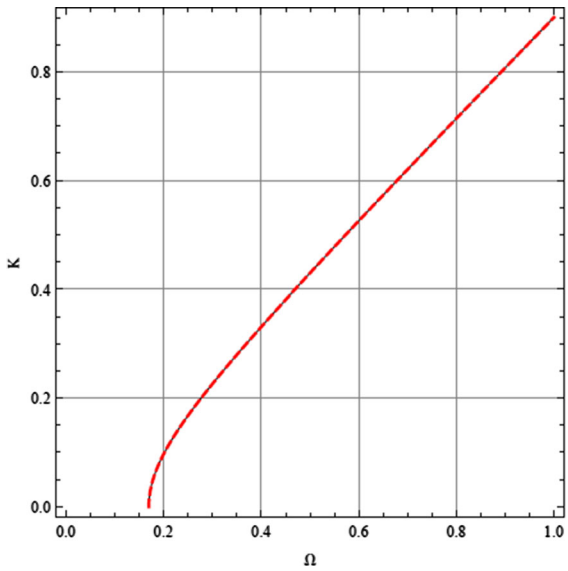

Fig. 4 Lowest dispersion branch for the exact (black solid line) and shortened polynomial (dashed red line) dispersion relations Eqs. (18) and (25). (Color figure online)

$$
\begin{aligned}
G_4 &= (-3\mu - 1)\nu - \frac{\mu}{2},\\
G_5 &= \left(\mu + \frac{1}{6}\right)\nu + \frac{\mu}{24} + \frac{2\nu^2}{3},\\
&\vdots
\end{aligned}
\tag{25}
$$

where from the present setup relation we get

$$h \sim 1, \quad \nu = \frac{\mu}{\rho} \sim 1.$$

Thus, we obtain the shortened polynomial dispersion relation as follows:

$$\mu + G_1 K^2 + G_2 K^4 + G_3 K^2 \Omega^2 + G_4 \Omega^2 + G_5 \Omega^4 = 0. \tag{26}$$

We, therefore, depict in Fig. 4 the lowest dispersion branch for the exact (black solid line) and the shortened polynomial (dashed red line) dispersion relations (18) and (25) for the following set of parameters $h = 1,\ \mu = 0.025,\ \rho = 0.03$.

5.2 Stiff thin skin layers, light outer core layers and stiff thin inner core layer ($\mu \ll 1,\ h \sim \mu,\ \rho \sim \mu^2$)

Using the present setup, the following asymptotic relation can be deduced from Eq. (23):

$$G_1 \sim G_2 \sim G_3 \sim G_4 \sim G_5 \sim 1, \tag{27}$$

and having in mind that higher orders of μ go to zero more faster, we obtain the following by retaining only μ^2 to feel the presence of κ,

$$
\begin{aligned}
G_1 &= \mu^2 + \mu + 1,\\
G_2 &= \mu^2 + \frac{7\mu}{24} + \frac{1}{3},\\
G_3 &= \left(-\frac{\kappa}{2} - \frac{1}{2}\right)\mu^2 - \frac{\mu}{3} - \frac{\nu}{4} - \frac{1}{6},\\
G_4 &= -\kappa\mu^2 - \frac{\mu}{2} - \frac{\nu}{2},
\end{aligned}
$$

$$G_5 = \frac{\kappa\mu^2}{2} + \frac{\mu}{24} + \frac{\nu^2}{2} + \frac{\nu}{4},$$
$$\vdots \tag{28}$$

where

$$h \sim \mu, \quad \kappa = \frac{h}{\rho} \sim 1, \quad \nu = \frac{\mu^2}{\rho} \sim 1.$$

Therefore, we obtain the shortened polynomial dispersion relation as follows:

$$\mu + G_1K^2 + G_2K^4 + G_3K^2\Omega^2 + G_4\Omega^2 + G_5\Omega^4 = 0. \tag{29}$$

We normalize the dimensionless frequency and wave number in Eq. (29) using the following:

$$K^2 = \mu\Upsilon^2 \quad \Omega^2 = \mu\Psi^2, \tag{30}$$

and thereafter making use of a near cut-off asymptotic expansion of the form

$$\Psi^2 = \Psi_0^2 + \mu\Psi_1^2 + \mu^2\Psi_2^2 + \cdots, \tag{31}$$

on Eq. (29) to further simply it to obtain

$$\begin{aligned}
\Psi_0^2 &= 0,\\
\Psi_1^2 &= 1 + \Upsilon^2,\\
\Psi_2^2 &= -\frac{\nu}{2} + \left(1 - \frac{\nu}{2}\right)\Upsilon^2 + \frac{\Upsilon^4}{3},\\
&\vdots
\end{aligned} \tag{32}$$

and yielding the optimal shortened dispersion relation below

$$K^2\left(-\frac{\mu^2\nu}{2} + \mu^2 + \mu\right) + \frac{\mu}{3}K^4 - \Omega^2 + \left(\mu^2 - \frac{\mu^3\nu}{2}\right) = 0. \tag{33}$$

Therefore, we depict in Fig. 5 the lowest dispersion branch for the exact (black solid line) and the shortened polynomial (dashed red line) dispersion relations (18) and (33) using the parameters $h = 1,\ \mu = 0.053,\ \rho = 0.0032$.

6 Asymptotic behaviour for the displacements and stresses

In this section, we study the asymptotic behaviours of the obtained displacements and stresses in the respective layers presented in Sect. 2.

To achieve the set objective, the following rescaling of

$$K^2 = \mu\Upsilon^2 \quad \Omega^2 = \mu\Psi^2,$$

into Eqs. (9)–(12) is necessary. We thus obtain to the asymptotic formulae:

$$\begin{aligned}
u_1 &= h_2 h\xi_{2_1},\\
\sigma_{13}^1 &= \mathrm{i}\mu_1\sqrt{\mu}\Upsilon h\xi_{2_1},\\
\sigma_{23}^1 &= \mu_1,\\
u_2 &= h_2\left(h + \frac{1}{\mu}\xi_{2_2}\right),\\
\sigma_{13}^2 &= \mathrm{i}\mu_2\sqrt{\mu}\Upsilon\left(h + \frac{1}{\mu}\xi_{2_2}\right),
\end{aligned} \tag{34}$$

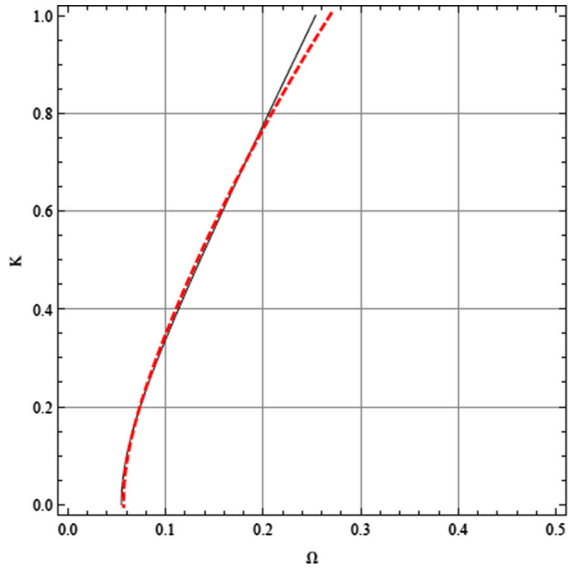

Fig. 5 Lowest dispersion branch for the exact (blue solid line) and shortened polynomial (dashed red line) dispersion relations Eqs. (18) and (33). (Color figure online)

$$\sigma_{23}^2 = \frac{\mu_2}{\mu}, \tag{35}$$

and

$$\begin{aligned} u_3 &= h_2 \left(h + \frac{1}{\mu}\right) \left(1 - \alpha_2^2 \left(h + 2\right) \left(\xi_{2_3} + h + 1\right)\right), \\ \sigma_{13}^3 &= \mathrm{i}\mu_1 \sqrt{\mu} \Upsilon \left(h + \frac{1}{\mu}\right) \left(1 - \alpha_2^2 \left(h + 2\right) \left(\xi_{2_3} + h + 1\right)\right), \\ \sigma_{23}^3 &= \mu_1 \alpha_2^2 \left(h + \frac{1}{\mu}\right) \left(\xi_{2_3} - 1\right), \end{aligned} \tag{36}$$

with

$$\alpha_2 = \sqrt{\mu \Upsilon^2 - \frac{\mu^2}{\rho} \Psi^2}. \tag{37}$$

We therefore deduce the mentioned asymptotic relation taking into account both the setups (i) and (ii) as follows:

$$\frac{u_1}{h_2 h} \sim \frac{\sigma_{13}^1}{\mu_1 \sqrt{\mu} h} \sim \frac{\sigma_{23}^1}{\mu_1}, \tag{38}$$

and

$$\frac{u_i}{h_2 N} \sim \frac{\sigma_{13}^i}{\mu_i \sqrt{\mu} N} \sim \frac{\sigma_{23}^i}{\mu_i}, \tag{39}$$

for $i = 2, 3$, where $\mu_1 = \mu_3$ as stated earlier, and

$$N = h + \mu^{-1}. \tag{40}$$

7 Conclusion

In summary, an asymptotic approach of study is used to analyze the antisymmetric anti-plane shear vibration of an elastic inhomogeneous five-layered plate. The plate under consideration consists of five alternating layers; precisely, two different layers arranged symmetrically to form an alternating five-layered plate. The exact displacements,

stresses and dispersion relation have been determined analytically after reducing the governing equations to ordinary differential equations with the help of the prescribed boundary and interfacial conditions. The obtained exact dispersion relation and its corresponding polynomial dispersion relation were investigated within the long-wave low-frequency region in favour of its vast applications. Furthermore, we have analyzed the both the exact and approximate dispersion relations by considering two contrasting material setups that are of industrial applications and corresponding to layered plates with light-stiff layer combinations [10–12]. In addition, some asymptotic formulae for the obtained exact displacement and stresses have been derived in each layer of the plate. It is remarkable that the contrasting material setup (i) is applicable over the whole low-frequency range; whereas (ii) is valid over a constricted vicinity of the range. This in fact is similar to the three-layered plate case [10]. However, it is interesting to note that more dispersion curves are noted here in distinction with [10] as shown in Fig. 3. Similarly, the recovery of the results in [10] can be realized upon setting $r = 1$ in Eqs. (20)–(21). Finally, it is recommended that a similar study should be carried out by considering strongly inhomogeneous layered plates in the presence of some structural or material discontinuities such as cracks or voids together with the influence of certain external excitations. Approximate equations of vibration can also be of interest in this regard.

Acknowledgements The second author, Rahmatullah Ibrahim Nuruddeen sincerely acknowledges the 2017 CIIT-TWAS Full-time Postgraduate Fellowship Award (FR Number: 3240299480).

Declarations

Conflict of interest The authors declare that they have no conflict of interest.

References

1. Achenbach JD (1999) Wave propagation in elastic solids. Eight impression. Elsevier, Amsterdam
2. Kaplunov JD, Kossovich LY, Nolde EV (1998) Dynamics of thin walled elastic bodies. Academic Press, San Diego
3. Altenbach H, Eremeyev VA, Naumenko K (2015) On the use of the first order shear deformation plate theory for the analysis of three-layer plates with thin soft core layer. ZAMM 95(10):1004–1011
4. Kaplunov J, Nobili A (2017) Multi-parametric analysis of strongly inhomogeneous periodic waveguides with internal cut-off frequencies. Math Methods Appl Sci 40(9):3381–3392
5. Craster R, Joseph L, Kaplunov J (2014) Long-wave asymptotic theories: the connection between functionally graded waveguides and periodic media. Wave Motion 51(4):581–588
6. Sahin O, Erbas B, Kaplunov J, Savsek T (2019) The lowest vibration modes of an elastic beam composed of alternating stiff and soft components. Arch Appl Mech 90(2):339–352
7. Sayyad AS, Ghugal YM (2017) Bending, buckling and free vibration of laminated composite and sandwich beams: a critical review of literature. Compos Struct 171:486–504
8. Naumenko K, Eremeyev VA (2014) A layer-wise theory for laminated glass and photovoltaic panels. Compos Struct 112:283–291
9. Lee P, Chang N (1979) Harmonic waves in elastic sandwich plates. J Elast 9(1):51–69
10. Kaplunov J, Prikazchikov D, Prikazchikova L (2917) Dispersion of elastic waves in a strongly inhomogeneous three-layered plate. Int J Solids Struct 113:169–179
11. Prikazchikov LA, Aydin YE, Erbaş B, Kaplunov J (2018) Asymptotic analysis of anti-plane dynamic problem for a three-layered strongly inhomogeneous laminate. Math Mech Solids 25(1):3–16
12. Erbas B (2018) Low frequency antiplane shear vibrations of a three-layered elastic plate. Eskişehir Techn University J Sci Techno A Appl Sci Eng 19(4):867–879
13. Kaplunov J, Prikazchikov DA, Sergushova O (2016) Multi-parametric analysis of the lowest natural frequencies of strongly inhomogeneous elastic rods. J Sound Vib 366:264–276
14. Kaplunov J, Prikazchikov DA, Prikazchikov LA, Sergushova O (2019) The lowest vibration spectra of multi-component structures with contrast material properties. J Sound Vib 445:132–147
15. Nuruddeen RI, Nawaz R, Zia ZQM (2020) Investigating the viscous damping effects on the propagation of Rayleigh waves in a three-layered inhomogeneous plate. Phys Scr 95(065224):1–11
16. Nuruddeen RI, Nawaz R, Zia ZQM (2021) Dispersion of elastic waves in an asymmetric three-layered structure in the presence of magnetic and rotational effects. Progr Electromag Res M 91:165–177
17. Belarbi MO, Tati A, Ounis H, Khechai A (2017) On the free vibration analysis of laminated composite and sandwich plates: a layerwise finite element formulation. Latin Am J Solids Struct 14(12):2265–2269
18. Assadi A, Najaf H (2020) Nonlinear static bending of single-crystalline circular nanoplates with cubic material anisotropy. Arch Appl Mech 90:847–868

19. Zhai Y, Li Y, Liang S (2018) Free vibration analysis of five-layered composite sandwich plates with two-layered viscoelastic cores. Solids Struct 200(15):346–357
20. López-Aenlle M, Pelayo F (2019) Static and dynamic effective thickness in five-layered glass plates. Solids Struct 212(15):259–270
21. Shishehsaz M, Raissi H, Moradi S (2019) Stress distribution in a five-layer circular sandwich composite plate based on the third and hyperbolic shear deformation theories. Mech Adv Mater Struct 26(14):927–940
22. Nuruddeen RI, Nawaz R, Zia ZQM (2020) Asymptotic analysis of an anti-plane shear dispersion of an elastic five-layered structure amidst contrasting properties. Arch Appl Mech 90:1875–1892
23. Talebitooti R, Johari V, Zarastvand M (2018) Wave transmission across laminated composite plate in the subsonic flow investigating two-variable refined plate theory. Lat Am J Solids Struct 15(5):1–18
24. Talebitooti R, Zarastvand MR, Gohari HD (2018) Investigation of power transmission across laminated composite doubly curved shell in the presence of external flow considering shear deformation shallow shell theory. J Vib Control 24(19):4492–4504
25. Talebitooti R, Zarastvand MR, Rouhani AHS (2019) Investigating hyperbolic shear deformation theory on vibroacoustic behavior of the infinite functionally graded thick plate. Lat Am J Solids Struct 16(1):1–17
26. Talebitooti R, Zarastvand MR, Darvishgohari H (2019) Multi-objective optimization approach on diffuse sound transmission through poroelastic composite sandwich structure. J Sandwich Struct Mater 12:1–20
27. Gohari HD, Zarastvand MR, Talebitooti R (2020) Acoustic performance prediction of a multilayered finite cylinder equipped with porous foam media. J Vib Control 26(11–12):899–912
28. Talebitooti R, Zarastvand MR, Gohari HD (2018) The influence of boundaries on sound insulation of the multilayered aerospace poroelastic composite structure. Aerospace Sci Techn 80:452–471
29. Zarastvand MR, Ghassabi M, Talebitooti R (2019) Acoustic insulation characteristics of shell structures: A review. Arch Comput Methods Eng. 1–19
30. Talebitooti R, Zarastvand M, Gheibi MR (2016) Acoustic transmission through laminated composite cylindrical shell employing third order shear deformation theory in the presence of subsonic flow. Compos Struct 157(1):95–110
31. Wang X, Shi G (2014) A simple and accurate sandwich plate theory accounting for transverse normal strain and interfacial stress continuity. Compos Struct 107:620–628
32. Talebitooti R, Khameneh AMC, Zarastvand MR, Kornokar M (2018) Investigation of three-dimensional theory on sound transmission through compressed poroelastic sandwich cylindrical shell in various boundary configurations. J Sandwich Struct Mater 21(7):2313–2357
33. Lawrie JB, Afzal M (2017) Acoustic scattering in a waveguide with a height discontinuity bridged by a membrane: a tailored Galerkin approach. J Eng Math 105(1):99–115
34. Talebitooti R, Gohari HD, Zarastvand MR (2017) Multi objective optimization of sound transmission across laminated composite cylindrical shell lined with porous core investigating non-dominated sorting genetic algorithm. Aerospace Sci Techn 67:269–280
35. Chang K, Wang W, Hsu S (2020) Antiplane response of a flat-bottomed semicircular canyon to cylindrical elastic waves. J Eng Math 121:125–139
36. Talebitooti R, Zarastvand MR (2018) The effect of nature of porous material on diffuse field acoustic transmission of the sandwich aerospace composite doubly curved shell. Aerospace Sci Techn 78:157–170
37. Ghassabi M, Zarastvand MR, Talebitooti R (2020) Investigation of state vector computational solution on modeling of wave propagation through functionally graded nanocomposite doubly curved thick structures. Eng Comp. 36:1417–1433
38. Demirkus D (2019) Antisymmetric dark solitary SH waves in a nonlinear heterogeneous plate. Z Angew Math Phys 70(173):1–11
39. Satti JU, Afzal M, Nawaz R (2019) Scattering analysis of a partitioned wavebearing cavity containing different material properties. Phys Scr. 94(11):115223
40. Talebitooti R, Zarastvand M (2018) Vibroacoustic behavior of orthotropic aerospace composite structure in the subsonic flow considering the third order Shear deformation theory. Aerospace Sci Techn 75:227–236
41. Demirkus D (2018) Non-linear bright solitary SH waves in a hyperbolically heterogeneous layer. Int J Non-Linear Mech 102:53–61
42. Ghassabi M, Talebitooti R, Zarastvand MR (2018) State vector computational technique for three-dimensional acoustic sound propagation through doubly curved thick structure. Comp. Methods Appl Mech Eng 352(1):324–344